J Mol Model (2010) 16:223–233
DOI 10.1007/s00894-009-0537-7

ORIGINAL PAPER

Mg-Al layered double hydroxide intercalated with porphyrin anions: molecular simulations and experiments

Petr Kovář · Miroslav Pospíšil · Eva Káfuňková · Kamil Lang · František Kovanda

Received: 9 April 2009 / Accepted: 10 June 2009 / Published online: 3 July 2009

Abstract Molecular modeling in combination with powder X-ray diffraction (XRD) provided new information on the organization of the interlayer space of Mg-Al layered double hydroxide (LDH) containing intercalated porphyrin anions [5,10,15,20-tetrakis(4-sulfonatophenyl)porphyrin (TPPS)]. Anion-exchange and rehydration procedures were used for the preparation of TPPS-containing LDH with an Mg/Al molar ratio of 2. Molecular modeling was carried out in the Cerius^2 and Materials Studio modeling environment. Three types of models were created in order to simulate the experimental XRD patterns of LDH intercalates with a TPPS loading of 70–80% with respect to the theoretical anion exchange capacity (AEC). The models represent single-phase systems with a 100% TPPS loading in the interlayer space (Type 1) and models represent the coexistence of two phases corresponding to the total exchange from 75 to 92% (Type 2). To cover other possible arrangements, models with the coexistence of both TPPS and NO_3^- anions in the same interlayer space were calculated (Type 3). The models are described and compared with experimental data. In all cases, guest TPPS anions are tilted with respect to the hydroxide layers, and are horizontally shifted to each other by up to one-half of the TPPS diameter. According to the energy characteristics and simulated XRD, the most probable arrangement is of Type 2, where some layers are saturated with TPPS anions and others are filled with original NO_3^- anions.

Keyword Layered double hydroxide · Porphyrin · Molecular simulations · Intercalation · X-ray diffraction

P. Kovář (✉) · M. Pospíšil
Faculty of Mathematics and Physics,
Charles University in Prague,
Ke Karlovu 3,
121 16 Prague, Czech Republic
e-mail: kovar@karlov.mff.cuni.cz

E. Káfuňková · K. Lang
Institute of Inorganic Chemistry, v.v.i,
Academy of Sciences of the Czech Republic,
250 68 Řež, Czech Republic

E. Káfuňková
Faculty of Sciences, Charles University in Prague,
2030 Hlavova,
128 43 Prague, Czech Republic

F. Kovanda
Department of Solid State Chemistry,
Institute of Chemical Technology,
Prague, Technická,
5 166 28 Prague, Czech Republic

Introduction

Layered double hydroxides (LDHs), known also as hydrotalcite-like compounds or anionic clays, are layered materials with a chemical composition represented by the general formula $\left[M^{II}{}_{1-x}M^{III}{}_{x}(OH)_2\right]^{x+}\left[A^{n-}{}_{x/n}\cdot yH_2O\right]^{x-}$ where M^{II} and M^{III} are divalent and trivalent metal cations, A^{n-} is n-valent anion, y is the number of water molecules, and x ranges usually between 0.20 and 0.33. The crystal structure is similar to that of brucite, $Mg(OH)_2$, where each Mg^{2+} cation is octahedrally surrounded by six hydroxyl groups and the adjacent octahedra share edges to form infinite sheets. The sheets are stacked and held together by non-bonded interactions. In the LDHs, the M^{II}/M^{III} isomorphous substitution in the octahedral sites of hydroxide

sheets results in a net positive charge that is compensated by anionic species localized together with water molecules in the interlayers.

A great number of LDHs with a variety of M^{II} and M^{III} cations in hydroxide layers and various interlayer anions have been reported. These materials have a wide range of applications, e.g., in polymer processing, heterogeneous catalysis, adsorption and decontamination processes, or pharmacy [1–4]. LDHs are often used as host structures for the loading of various organic anions. New applications of organic/inorganic hybrid materials based on intercalated LDHs have been proposed during the last decade, including analytical chemistry, electrochemistry, photochemistry (modified electrodes, sensors, etc.) [1, 5], pharmaceutical and biomedical applications (drug carriers, gene therapy) [2, 6, 7], or preparation of novel LDH/polymer nanocomposites [2, 8, 9]. In research and development of these hybrid materials, computer simulations represent a useful tool for obtaining an insight into the arrangement, properties, and dynamic behavior of interlayer organic species [10].

Molecular simulations allow information to be obtained about the structure and mutual interactions among constituents, including energy characteristics. Detailed descriptions of the interlayer structure, orientation and arrangement of interlayer species with respect to inorganic layers, and the influence of interlayer water molecules have been reported, e.g., citrate in LDH [11] or amino acids, phenylalanine, and tyrosine in LDH and montmorillonite [12]. Such simulations result in a more precise description of intercalated products compared to models based on stereochemistry and experimental data [13], allowing better understanding of individual interactions [14]. As the distribution and orientation of water molecules in the interlayer space are important factors for the resulting properties and arrangement of interlayer anionic species, the presence of water molecules cannot be neglected [10, 15, 16].

LDHs are characterized by relatively weak bonding between interlayer anions and hydroxide sheets, and these anions can be exchanged under suitable conditions. As carbonate anions show high affinity to hydroxide sheets, their replacement by anion exchange is very difficult. Therefore, the synthesis of LDHs containing specific interlayer anions requires carbonate- and CO_2-free conditions. By contrast, interlayer Cl^- and NO_3^- anions can be exchanged easily, and the chloride and nitrate forms of LDHs are often used as precursors in anion-exchange reactions. An alternative procedure is the rehydration of mixed oxides obtained by thermal decomposition of LDHs containing volatile interlayer anions (e.g., CO_3^{2-} or NO_3^-). During heating of Mg-Al-CO_3 LDHs, interlayer water is released below 200 °C [1]. The dehydroxylation of hydroxide layers and the loss of interlayer carbonate take place at higher temperatures (350–450 °C) followed by the collapse of the layered crystal structure to Mg–Al mixed oxides. These mixed oxides prepared at moderate calcination temperatures of 400–600 °C can be rehydrated in water. The rehydration process results in the reconstruction of the original layered structure, where compensating anions are anions dissolved in solution. Both anion-exchange and rehydration procedures can be used for intercalation of the desired anionic species into the LDH hosts.

The intercalation of intercalated porphyrin anions has practical consequences as [5,10,15,20-tetrakis (4-sulfonatophenyl)porphyrin (TPPS)] can be excited by visible light, and the formed porphyrin triplet states interact rapidly with oxygen molecules by energy transfer leading to the formation of singlet oxygen $^1O_2$. Singlet oxygen is a highly reactive oxidation agent and it is generally accepted that $^1O_2$ [mostly $O_2(^1\Delta_g)$] is the main cytotoxic species in photodynamic therapy of cancer [17]. In our previous work, we described the structural and photophysical properties of LDH powders and oriented films with intercalated porphyrin sensitizers [5, 18]. We have shown that the behavior of the porphyrin triplet state in LDHs is similar to that in solution. The possibility of fabricating LDH-based films, the reactivity, and short lifetime of $^1O_2$ suggest that these hybrids are suitable for the construction of photoreactive surfaces, especially those with bactericidal properties.

The present work focuses on Mg–Al LDH intercalated with TPPS. The arrangement of similar structures was studied using various experimental and calculation techniques. For example, the basal spacing and the size of guest dianions were compared using semi-empirical molecular orbital calculations. The results revealed the fact that guest anions act as a bridge between two adjacent LDH layers, and the relationship between the anion size (terephthalate, 2,6-naphthalenedisulfonate, 1,5-naphthalenedisulfonate, and 2,7-naphthalenedisulfonate) and interplanar spacing [19, 20]. In the case of tetrasulfonated porphyrin intercalates, their perpendicular orientation with respect to the LDH layers was suggested [13, 21]. The shape of the porphyrin molecule is crucial because static and dynamic optical properties change consistently with the increase in the nonplanarity of the porphyrin macrocycle. This nonplanarity can give rise to polar excited states, affecting charge transfer processes. It is noteworthy that a macroscopic dipole moment may occur even when a distorted macrocycle is highly symmetric, and even in the absence of central metal effects [22]. All the above mentioned influences were taken into consideration for TPPS characterization and calculations.

Experimental methods

Preparation of samples

The tetrasodium salts of TPPS (Aldrich, St. Louis, MO), $Mg(NO_3)_2{\cdot}6H_2O$, $Al(NO_3)_3{\cdot}9H_2O$ and NaOH (all Penta, Prague, Czech Republic) were used as purchased.

Synthesis of Mg–Al LDH hosts

The hydrotalcite-like host in the nitrate form was prepared by coprecipitation. Aqueous solution (450 ml) of Mg and Al nitrates with an Mg/Al molar ratio of two and a total metal ion concentration of 1.0 mol l^{-1} was added at a flow rate of 7.5 ml min^{-1} to a 1,000 ml reactor containing 200 ml distilled water. The flow rate of simultaneously added 3 M NaOH was controlled to maintain a pH value of 10.0±0.1. Carbonate-free distilled water was used for dissolution of components and the reaction was carried out under nitrogen to avoid any contamination of the product with carbonate anions. Coprecipitation proceeded under vigorous stirring at 75 °C and the resulting suspension was stirred for 1 h at 75 °C. The product was filtered off, washed several times with carbonate-free distilled water, and dried at 60 °C. The obtained product was denoted as $Mg_2Al–NO_3$ based on the Mg/Al molar ratio of Mg and Al nitrates in the solutions used.

Anion exchange

The LDH precursor $Mg_2Al–NO_3$ was dispersed in a carbonate-free aqueous solution (400 ml) of TPPS (0.001 M, pH 9 adjusted by 3 M NaOH). After mixing the components, the suspension was sealed in a 500 ml glass bottle under nitrogen and stirred for 6 days at 30 °C. The intercalated product was filtered off, washed with carbonate-free distilled water, and dried at 60 °C. The LDH host/porphyrin molar ratio was adjusted to achieve 100% loading with respect to the theoretical anion-exchange capacity (AEC) using a 10% molar excess of porphyrin. The product was denoted as Mg_2Al/TPPS-AE.

Rehydration procedure

The LDH precursor $Mg_2Al–NO_3$ was heated for 4 h at 450 °C in air and then cooled in a desiccator to room temperature. The Mg-Al mixed oxide obtained was dispersed under nitrogen in 75 ml of a carbonate-free aqueous solution of TPPS (0.001 M, pH 9 adjusted by 3 M NaOH) and placed in a 100 ml Teflon-lined stainless steel bomb. The rehydration reaction was carried out under hydrothermal conditions at 120 °C and autogenous pressure for 20 h. The rehydrated product was filtered off, washed with carbonate-free distilled water, and dried at 60 °C. The Mg–Al mixed oxide/porphyrin molar ratio was adjusted to achieve 100% loading with respect to the theoretical AEC of the resulting LDH, using a 10% molar excess of TPPS. The sample obtained was labeled by Mg_2Al/TPPS-R.

Characterization of the products

The phase composition of the prepared products was determined by powder X-ray diffraction (XRD) using a Siemens D5005 diffractometer (Bruker AXS, Karlsruhe, Germany) with Cu K_α radiation (λ=0.1542 nm, 40 kV, 30 mA, diffracted beam monochromator) in the 2θ range (2–80°, step size 0.02°,10s/point). The qualitative analysis was performed with the HighScore software package (PANalytical, Almelo, the Netherlands, version 1.0d), Diffrac-Plus software package (Bruker AXS, version 8.0), and JCPDS PDF-2 database. The magnesium and aluminum content was determined by volumetric analysis after dissolution of the samples in concentrated sulfuric acid. The content of intercalated porphyrin was estimated using UV-vis spectroscopy by measurement the absorption spectra of solutions before and after the intercalation process on a PerkinElmer Lambda 35 spectrometer. The content of interlayer water was estimated using the thermal analysis (simultaneous TGA/DSC/DTA QMS) on a NETZSCH apparatus STA 409 coupled with a quadrupole mass spectrometer Balzers QMG 420 (air atmosphere with a flow rate of 75 ml/min, heating rate of 10 K/min, gaseous products, i.e., 18-H_2O^+, 44-CO_2^+, and 46-NO_2^+ were continually monitored).

Molecular modeling

Molecular mechanics and classical molecular dynamics [23] were carried out in the Cerius^2 and Materials Studio modeling environment [24]. The host framework of $Mg_2Al–NO_3$ is a trilayered structure with a trigonal cell in hexagonal axes. The space group is R-3m. The cell parameters a=b=3.046 Å were determined from experimental XRD patterns. The layer of the composition $[Mg_{32}Al_{16}(OH)_{96}]^{16+}$ with a total charge of +16 is composed of 48 linked individual cells (lattice parameters: A=18.276 Åand B=24.368 Å) with Al cations distributed regularly on condition that the location of Al cations in neighboring octahedra is excluded [25].

The basal spacing of the initial models was set to the mean value obtained from the experimental XRD data (d_{003}= 22.1 Å, see below). Porphyrin TPPS was built in the 3D-Sketcher module [24]. Sazanovich et al. [22] reported a geometry of porphyrin derivatives from a semiempirical

point of view; the geometry and optical properties were investigated by successive addition of ethyl substituents at beta-pyrrole positions of free-base 5,10,15,20-tetraphenyl porphyrin (TPP). Semiempirical calculations indicated that the TPP molecule has a planar geometry. We started calculations using various force fields (Universal, Dreiding, Cff, Pcff) [26–30]. Porphyrin TPPS was built by the adding of SO_3^- groups at the *p*-positions of the phenyl rings, and the optimized planar geometry of TPPS used for subsequent calculations was obtained in the Dreiding force field parameters, which were able to maintain the planar geometry. The distance between two neighboring sulfur atoms of SO_3^- groups in TPPS is of 13.4 Å and the diagonal distance between two sulfur atoms is 19.0 Å.

The number of water molecules and TPPS tetraanions intercalated into the interlayers was determined by experimental measurements. Based on thermogravimetry, we estimated the water content to be 3.6–4.5 water molecules per $[Mg_4Al_2(OH)_{12}]^{2+}$ unit. Therefore, our models contained four water molecules per $[Mg_4Al_2(OH)_{12}]^{2+}$, which corresponds to the reported amount of interlayer water in the LDH precursor [3]. The analysis of TPPS solutions before and after intercalation procedures indicated that the achieved TPPS loading with respect to the theoretical AEC was approximately 70–80% [5].

Costantino et al. [31] and Miyata [32] reported the preparation and properties of LDHs containing various loadings of organic anions in the interlayer space. They showed that increasing the loading of organic anions in the interlayer results in changes in the positions and intensities of diffraction lines in powder XRD patterns. Since the TPPS loading in investigated samples was up to about 80% of AEC, we built three types of structure models. The aim was to obtain the optimized geometries and, by comparing the experimental and calculated X-ray diffraction patterns of the models, to address the most probable porphyrin orientations in real samples.

Type 1: The structure models have 100% TPPS loading in the interlayer space. A set of models with various orientations of guest porphyrin anions with respect to each other and to the LDH layers was created containing water molecules localized near the LDH layers. The total composition of the supercell was $Mg_{96}Al_{48}(OH)_{288}(TPPS)_{12}{\cdot}96H_2O$.

Type 2: These models represent a coexistence of two phases, with an overall TPPS loading of 75, 83, and 92%. For this purpose, we created a supercell consisting of 12 hydroxide layers with 9, 10, or 11 interlayers completely exchanged for TPPS anions respectively, while the remaining interlayers contained original NO_3^- anions. The d_{003} basal spacing of the nitrate LDH precursor was set to the value of 8.77 Å. The cell parameters of the investigated supercells were: A=18.276 Å, B=24.368 Å; the C parameter depended on the total TPPS loading. The total compositions and C values of the supercells were as follows: $[Mg_{384}Al_{192}(OH)_{1152}][(TPPS)_{36}(NO_3)_{48}{\cdot}384\ H_2O]$ and $C = (9 \times 22.1 + 3 \times 8.77) = 225.21$ Å, $[Mg_{384}Al_{192}(OH)_{1152}][(TPPS)_{40}(NO_3)_{32}{\cdot}384\ H_2O]$ and $C = (10 \times 22.1 + 2 \times 8.77) = 238.54$Å, and $[Mg_{384}Al_{192}(OH)_{1152}][(TPPS)_{44}\ (NO_3)_{16}{\cdot}384\ H_2O]$ and $C = (11 \times 22.1 + 8.77) = 251.87$Å for supercells with a TPPS loading of 75, 83, and 92 %, respectively. We created models with various interlayer sequences, e.g., TPPS, NO_3^-, TPPS, TPPS, NO_3^-, etc., and models representing two segregated phases loaded with TPPS and NO_3^- (i.e., the sequences TPPS, TPPS,..., NO_3^-, NO_3^-,...). In the latter case, the models consisted of 9 and 10 successive interlayer regions with TPPS and the remaining successive interlayers were saturated by NO_3^-. This corresponds to a total TPPS loading of 75 and 83 %, respectively.

Type 3: The models suggest the coexistence of both TPPS and NO_3^- anions in each interlayer space. Thus, the models corresponding to the total 75% TPPS loading contained three TPPS tetraanions, and the remaining positive layer charge was compensated by four NO_3^- anions. Models with various orientations of TPPS anions with respect to each other and to the hydroxide layers were created and NO_3^- anions were distributed randomly. The composition of the final supercell was $Mg_{96}Al_{48}(OH)_{288}(TPPS)_9(NO_3)_{12}{\cdot}96H_2O$ with the lattice supercell parameters A=18.276 Å, B=24.368 Å, and $C = 3 \times d_{003} = 66.3$Å.

To be able to describe all the atoms in the models and the energy characteristics, the initial models were minimized in the Universal force field. Charges were calculated using the Qeq method (charge equilibrium approach) [33], the electrostatic energy was calculated using the Ewald summation method [34], and the van der Waals energy was calculated using the Lennard-Jones potential [35].

Minimization was carried out in the Minimizer module according to the following strategy: first, the minimization of the models with 100% loading of TPPS in the interlayer was carried out (Type 1) to obtain the optimized positions of the guests with respect to the host layers. These arrangements were later used in the models of Type 2. LDH layers were kept as rigid units during the energy minimization. The cell parameters c, α, and β were variable, which allowed the mutual position of individual

layers to be refined, and the calculations to be accelerated. In the case of the Type 2 models, the cell parameters and the atoms of the host layers, except for hydrogen atoms of the OH groups were kept fixed during energy minimization. All positions of atoms in the interlayer were variable. The minimization strategy in the Type 3 models was the same as in the case of Type 1. The geometry of the minimized models was then refined by quench dynamics, a type of dynamics simulation where new arrangements of the interlayer space are generated. After a given number of dynamics steps the structure model is minimized, allowing elucidation of the dependence of the total crystal energy on the arrangement of the species in the interlayer space and their geometry. It helps to determine the most probable interlayer arrangement. The dynamics simulations were carried out in an NVT statistical ensemble (N = constant number of atoms, V = constant volume, T = constant temperature) at 300 K. One dynamic step was 0.001 ps and 70–100 ps of dynamics were carried out. During quench dynamics, all positions of atoms in the interlayer space and hydrogen atoms of the hydroxide OH groups were variable, while the positions of the remaining atoms in the layers were kept fixed. After that, the selected partially minimized structures were minimized to obtain the final structure models.

Results and discussion

Characterization of the prepared samples

Chemical analysis of the $Mg_2Al–NO_3$ precursor showed that the Mg/Al molar ratio corresponds to that adjusted in nitrate solutions used for coprecipitation. The chemical formula $Mg_{2.03}Al_{1.00}(OH)_{6.06}(NO_3)\cdot 1.2H_2O$ was determined from the results of chemical and thermal analysis. In the powder XRD patterns of the coprecipitated $Mg_2Al–NO_3$ sample, only a well-crystallized hydrotalcite-like phase, as indicated by the hexagonal lattice of the rhombohedral symmetry, was found (Fig. 1). The successful intercalation of bulky porphyrin anions into the LDH interlayer space was confirmed by a marked shift of the basal (003) diffraction line towards lower diffraction angles, i.e., the d_{003} value increased from 8.77 to 22.1 Å for $Mg_2Al–NO_3$ and Mg_2Al/TPPS-AE, respectively (Fig. 1). Similarly, the other basal diffraction lines, e.g., (006), were shifted.

Rehydration of the calcined Mg_2Al-NO_3 precursor resulted in the formation of the corresponding hydroxide form (Mg_2Al-OH). This phase of the chemical composition $Mg_{1.98}Al_{1.00}(OH)_{5.96}(OH)\cdot mH_2O$ is characterized by a d_{003} basal spacing of 7.63 Å. The intercalated phase with d_{003} of 21.4 Å together with the admixture of the Mg_2Al-OH phase

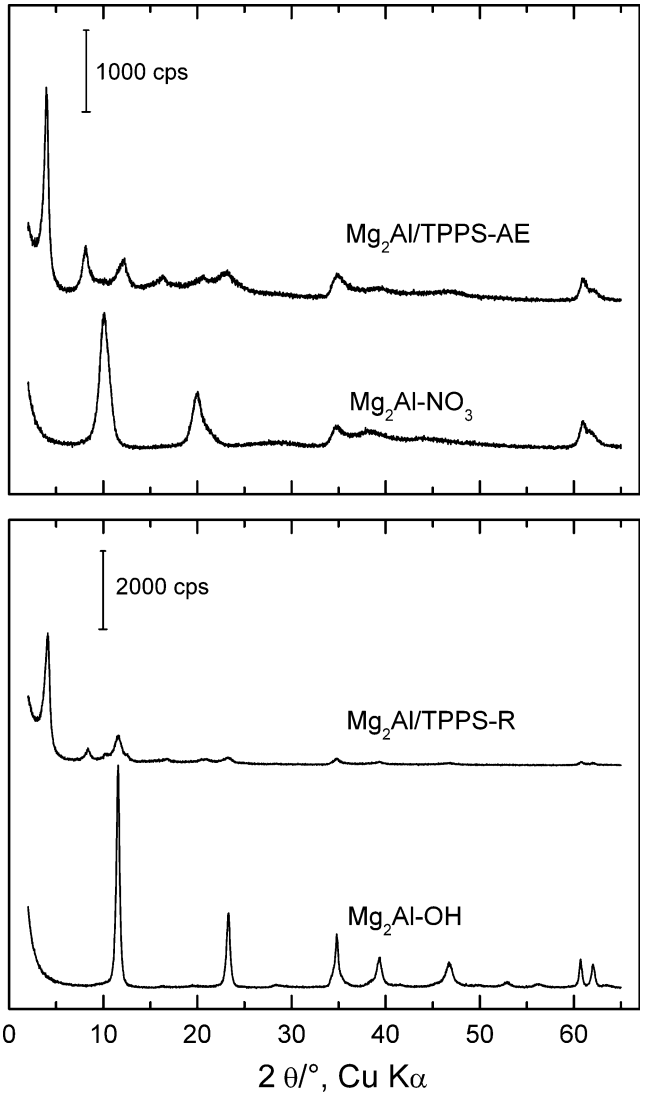

Fig. 1 Powder X-ray diffraction (XRD) patterns of Mg-Al layered double hydroxide (LDHs) intercalated with 5,10,15,20-tetrakis (4-sulfonatophenyl)porphyrin (TPPS) by anion exchange (AE) and rehydration (R) procedures: *Mg_2Al-NO_3* coprecipitated sample for anion exchange, *Mg_2Al-OH* product obtained by rehydration of calcined Mg_2Al-NO_3 sample in distilled water, *Mg_2Al/TPPS* intercalated products obtained using concentration conditions for 100% porphyrin loading with respect to the theoretical anion exchange capacity (AEC)

were found in the samples rehydrated in porphyrin-containing solutions (Fig. 1). The d_{003} value of the intercalated phase was close to that determined for the sample prepared by anion exchange. Evidently, during the rehydration process hydroxide anions in the interlayer space of the rehydrated product are substituted by porphyrin anions. The rehydrated samples exhibited slightly lower TPPS loading (about 70%). The presence of the parent nitrate LDH phase in Mg_2Al/TPPS-R is in accordance with the measured TPPS loading of 70 % with respect to AEC.

The orientation of porphyrin anions within the interlayer space can be roughly estimated by comparing the interlayer distance with the size of porphyrin molecules. Taking into account the thickness of the hydroxide sheet (~ 4.8 Å), the interlayer distance corresponds to about 17 Å. The adjacent sulfur atoms of TPPS are separated by about 13.4 Å and the most remote oxygen atoms of the adjacent SO_3^- groups are about 16.3 Å away. In addition, water molecules forming organized sheets close to the polar hydroxide surfaces contribute to the measured basal spacing [36]. The proportions indicate that two adjacent sulfonate groups of porphyrin anions interact with a hydroxide sheet via the hydroxyl groups of the positively charged sites. The opposite hydroxide sheet compensates for two remaining sulfonate groups. We have carried out the molecular modeling calculations using the parameters of the prepared LDH phases. The agreement between measured and calculated XRD diffraction lines of simulated systems allows for obtaining detailed information on the orientation of porphyrin moieties with respect to the hydroxide sheets, on the structure of porphyrin anions upon interaction with hydroxide sheets, and on the relative stability of the phase with mixed intercalated anions (i.e., Type 3). The results obtained are discussed below in more detail.

Molecular modeling

Molecular simulations combined with XRD resulted in a potential arrangement of the guest anions in the interlayer space and provided insights into the energy characteristics and location of water molecules. The calculated powder XRD patterns of the models representing one phase and the models representing the coexistence of two phases are described and compared with the experimental measurements in Fig. 2. The LDH basal diffraction lines were present at intervals of 2θ from 3 to 25°. Because the XRD module used does not take into account the roughness and bending of the hydroxide layers (the LDH layers were kept as rigid bodies), the calculated XRD patterns exhibit lower relative intensities of diffraction lines in comparison with the measured lines.

Single-phase models (Type 1 and Type 3)

Before discussing the XRD diffraction patterns, we will address possible horizontal arrangements of TPPS anions in the interlayer space. Calculations were performed for both Type 1 and Type 3 models. We present the three most different arrangements. The top views of the linked cells of Type 3 are presented in Figs. 3, 4, and 5. The arrangement A in Fig. 3 is characterized by the following features: (1) the porphyrin moieties tend to be parallel to each other with approximately ±10° variability; (2) the porphyrin moieties

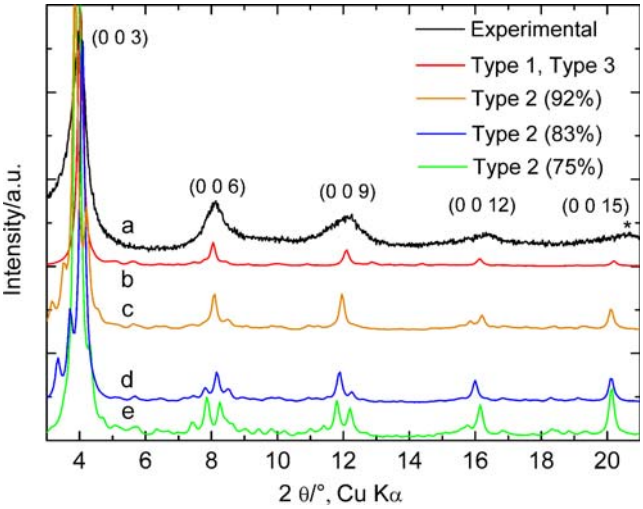

Fig. 2 Powder XRD patterns of Mg_2Al/TPPS-AE: comparison of experimental (*a*, impurity is labeled by *) and calculated XRD for single-phase (Type 1 and Type 3; *b*) and two-phase models (Type 2) with 92 (*c*), 83 (*d*) and 75% (*e*) exchange

are horizontally shifted by about 6 Å, i.e., approximately one-half of the TPPS anion size; and (3) the arrangement of TPPS anions in the interlayer space is disordered. The alternative arrangement B (Fig. 4) shows that (1) guest TPPS anions are more ordered than in A, (2) TPPS are arranged in rows following the [110] crystallographic direction, and (3) the guest anions are parallel and horizontally shifted similar to arrangement A (about 6 Å). Arrangement C (Fig. 5) has disordered rows of guest anions with variations in the mutual horizontal shift equal to about one-fourth of the TPPS anion size (4 Å). In all cases the remaining positive charges are compensated by NO_3^- located near the hydroxide layers. The sublimation energies per single interlayer are given in Table 1. The energy characteristics, i.e., electrostatic and van der Waals interactions, and the total energies differ only slightly (<1%). Therefore, all three arrangements can be adopted with the same probability, and a combination in which each interlayer was filled with the different arrangement in the sequence A, B and C was used for subsequent calculations. In the case of Type 1 models, the sublimation energy values per one interlayer differ in the range of 9% and therefore the arrangement A in Fig. 3 is more probable than those in Figs. 4 and 5. The powder XRD patterns of the Type 3 model are similar to experimental data (Fig. 2, traces a and b).

The calculated XRD patterns of Type 1 are characterized by five sharp basal diffraction lines (003), (006), (009), (0012) and (0015) in the 2θ interval from 3 to 25° (Fig. 2b) and match the measured patterns. The corresponding side view of the interlayer arrangement of porphyrin anions in the Mg_2Al-lattice with a d_{003} basal spacing of 22.2 Å is shown in Fig. 6a. The guest anions are not arranged perpendicularly with respect to the hydroxide sheets. The

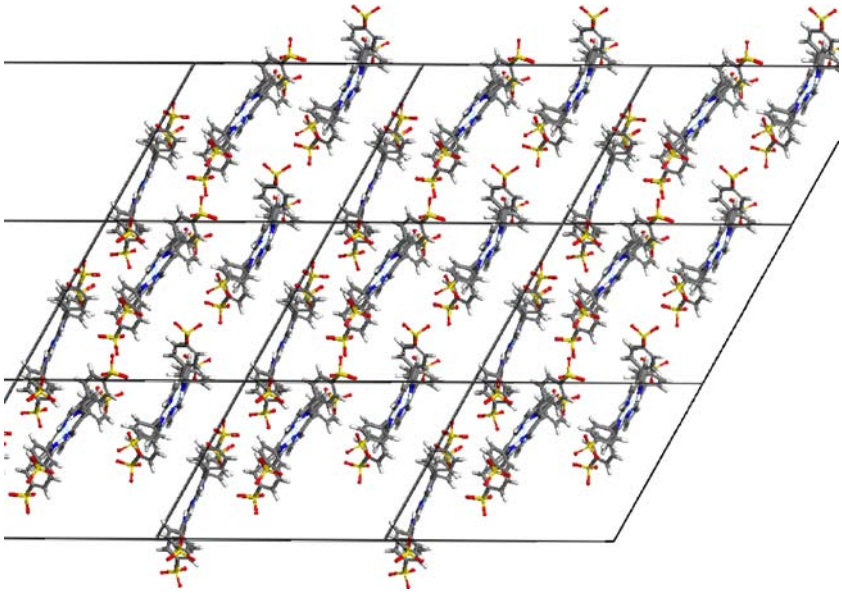

Fig. 3 Top view of linked cells describing a disordered arrangement of TPPS anions (Arrangement A)

tilted angle measured between the host layer and tangent of the pyrrole units ranges from 53 to 63°. For comparison, Fig. 6b shows an example of the arrangement of the Type 3 model containing the single phase with 75% TPPS loading. Here, the porphyrin units are tilted less from the layer normal due to a lower concentration of TPPS, and the angle between the host layer and porphyrin planes ranges from 68 to 71°.

The relative energy of repulsive interactions between TPPS anions is of 343±13 kcal mol^{-1} per TPPS, and between TPPS and NO_3^- is of 347±17 kcal mol^{-1} per TPPS (Type 3). In addition, the attractive interactions between TPPS anions and the layers are 1,844± 63 kcal mol^{-1} per TPPS. The attractive interactions between TPPS anions and the layers in Type 1 models are 1,842±63 kcal mol^{-1} per TPPS. However, the models differ in the repulsive energy between the guest anions as this energy is about two times higher than in the case of Type 3. Evidently, this is because of the closer distance between TPPS moieties (ca. 5 Å) than in the Type 3 model (i.e., 6–8 Å). The higher repulsive interactions of the guests explain the differences between the tilted angles of the TPPS planes. The powder XRD patterns of the two models are very similar; therefore, only one XRD is shown in Fig. 2.

Two-phase models (Type 2)

The powder XRD patterns of the Type 2 model containing the interlayers saturated either with NO_3^- (L-NO3) or with TPPS (L-TPPS) anions are compared with those of the single-phase models in Fig. 2. The effect of the increasing total loading with TPPS anions on the XRD profiles is

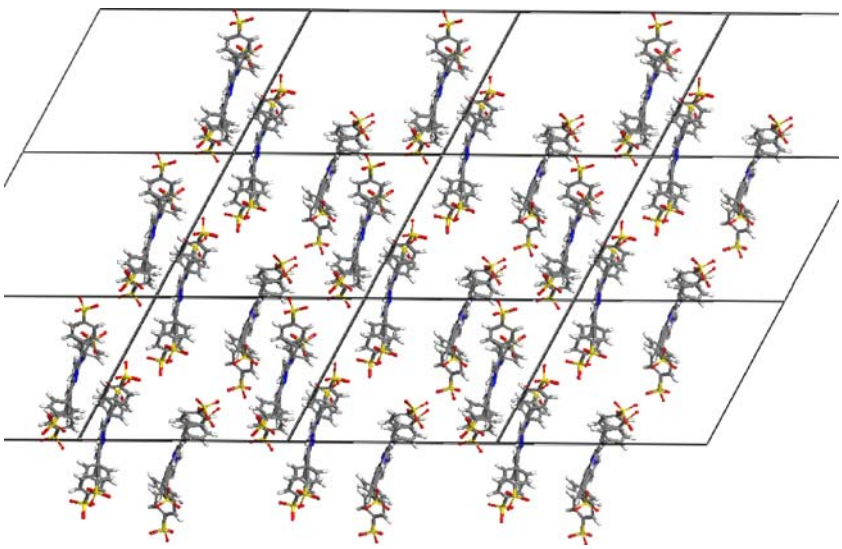

Fig. 4 Top view of an ordered arrangement of TPPS anions into the rows that follow the [1 1 0] direction (Arrangement B)

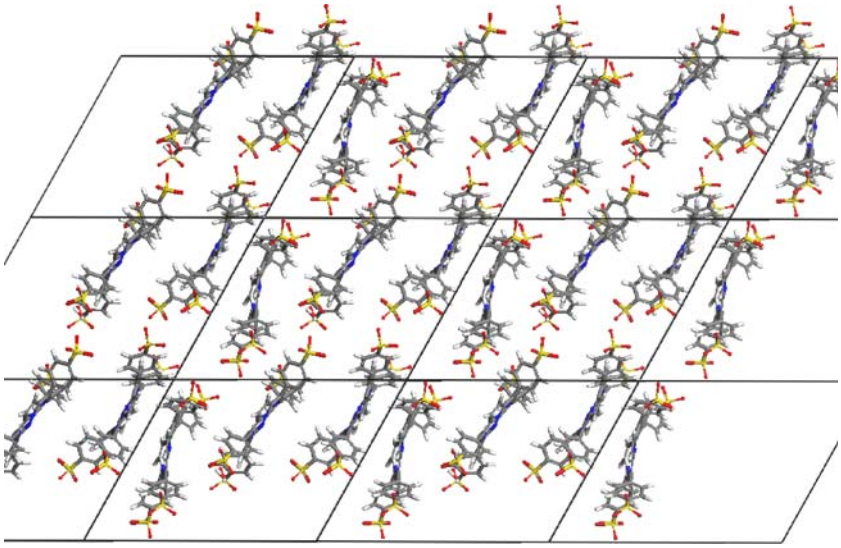

Fig. 5 Top view of an arrangement of TPPS anions into the rows that follow the [1 0 0] direction (Arrangement C)

evident. The calculated XRD patterns belong to the models containing a fully saturated part, with TPPS segregated from the non-exchanged part containing NO_3^-. The sequences with random alternation of individual interlayers (e.g.,...,TPPS, NO_3^-, TPPS, TPPS, NO_3^-,...) exhibit considerable differences from the measured XRD patterns. Therefore, we have focused predominantly on consecutive sequences with a various number of individual interlayers (e.g.,...TPPS, TPPS, NO_3^-, NO_3^-,...).

In all cases, the powder XRD patterns are characterized by a sharp and intensive (003) diffraction line at 2θ ranging from 3.9 to 4.1° depending on the calculated model. These 2θ values correspond to the basal spacing values ranging from 21.7 to 22.8 Å, and are quite similar to the experimental value of 22.1 Å. The presence of non-exchanged LDH interlayers causes a splitting of the diffraction lines due to a mixing of the interlayers (L-TPPS, L-NO3) on the nanometer scale. This is especially obvious for the diffraction lines around 8° and 12°, which are labeled as (0 0 6) and (0 0 9) in the single-phase models, respectively. In the case of Type 2 (75%), the supercell with 12 interlayers containing 9 L-TPPS and 3 L-NO_3 interlayers leads to the splitting of the diffraction line (0 0 6) into two at 2θ of 7.9 and 8.3°. Similarly, the line (0 0 9) splits into two at 11.8 and 12.2°. The splitting of (0 0 3) line (2θ=4.3°) also occurs. The model Type 2 (83%) (10 L-TPPS+2 L-NO_3) is characterized by the central line with 2θ of 8.2° that is close to the (0 0 6) line of the single-phase models and by two symmetrically localized peaks. The line at 2θ=11.9° is surrounded by a weak line at 12.2°. The line with 2θ of 4.1° exhibits the additional contribution of lines at 3.3 and 3.7°. On the contrary, there is no influence of the non–exchanged layer in the Type 2 (92%) composed of 11 L-TPPS and 1 L- NO_3^- on the positions of the lines at 2θ of 8.1 and 12.0°. These are very similar to the (0 0 6) and (0 0 9) lines of the single-phase models. The intensive diffraction line at 3.9 is accompanied by the low intensity peaks at 3.2 and 3.5° similarly to Type 2 (83%).

Summing up, the presence of two phases can contribute to the broadening of the diffraction lines. If we compare the calculated XRD patterns, it is clear that both single-phase (i.e., Type 1 and Type 3) and two-phase (i.e., Type 2) models are possible. The observed broadening in the experimental XRD lines is determined by the low crystallinity of the samples that is a typical feature of coprecipitated LDHs composed of Mg and Al, thus overlapping the possible split of the diffraction lines. Since the structural calculated models are perfectly periodic, the broadening of the peaks is not observed in the calculated patterns.

While the comparison of calculated and experimental XRD patterns cannot give an explicit distinction between single- and two-phase models, the values of sublimation energy offer solid arguments. We compared the total sublimation energy of the single-phase model [12-layered supercell with a mixture of 3 TPPS and 4 NO_3^- anions in each interlayer space (Type 3) with that of the two-phase model having the same TPPS loading (Type 2; 75%)]. The total sublimation energies for the Type 3 and Type 2 (75%) models are −46,780 kcal mol^{-1} and −116,960 kcal mol^{-1},

Table 1 Sublimation energy characteristics (van der Waals (vdW) and electrostatic interactions and their sum per TPPS) of three arrangements of the guests for the Type 3 model

Arrangement	E_{total}/ kcal/ mol	vdW/ kcal/ mol	Electrostatic/ kcal/ mol
A	-1,258	-38	-1,220
B	-1,232	-37	-1,195
C	-1,209	-39	-1,170

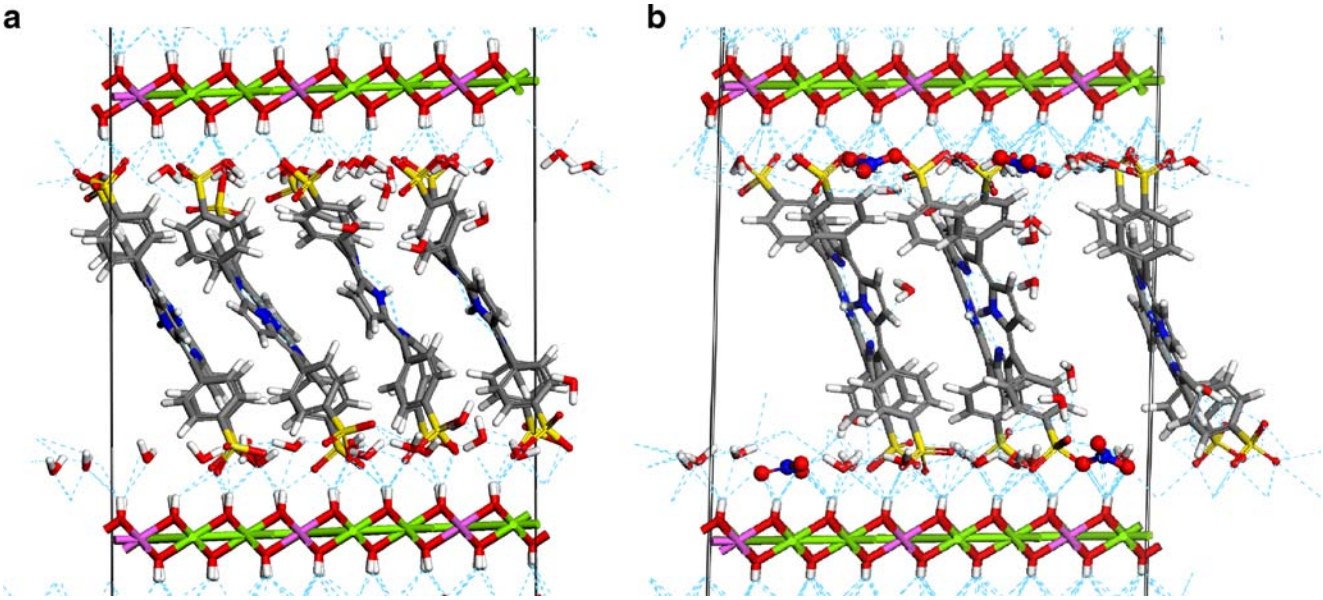

Fig. 6 Side view of the interlayer space in the Mg_2Al-lattice of Type 1 (**a**) and of Type 3 with NO_3^- anions located near LDH layers (**b**). *Blue lines* Hydrogen bonds

respectively. This indicates that the Type 2 model is more favorable than mixed anions in interlayers. Based on these arguments we suggest that the partial exchange of original anions in real samples leads to consecutively arranged interlayers filled with TPPS anions followed by others containing only original NO_3^- anions.

Geometry of TPPS anions

In general, the original flat moiety of TPPS anions (Fig. 7a) changes during dynamics simulations depending on the mutual arrangement of the guest anions, their location in the interlayer space, and the angle of tilt with respect to the host layers. There is continuous variation between two limited cases: the porphyrin moieties remain nearly planar, with small deviations from the original planar geometry (Fig. 7b), or are settled into the saddle conformation (Fig. 7c). In both cases, the phenyl rings with SO_3^- groups do not exhibit any significant bending or twisting with respect to the original porphyrin geometry. The models containing deviated guest anions in the interlayer space exhibit slightly different total energy when compared with the models based on nearly planar TPPS structure. Thus, from an energy point of view, the original planar geometry of TPPS anions might deviate after porphyrin interactions with the hydroxide sheets within the interlayer space. The water molecules are located near the hydroxide layers. In the presence of a lower concentration of TPPS (Type 3), a small amount of water (five molecules per supercell) can be located between the porhyrin cores and can interact with the pyrrols via hydrogen bonds. In the case of full saturation with TPPS anions, water molecules are located near the hydroxide layers.

Conclusions

Molecular simulations were used to describe the arrangement of the interlayer space of Mg-Al LDH intercalated

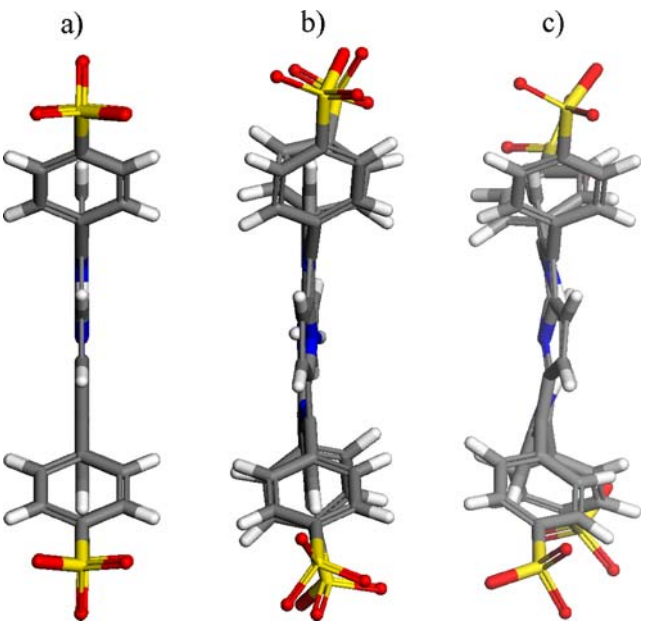

Fig 7a–c Geometry of TPPS. Original flat moiety (**a**) and two limited cases in the interlayer space obtained by molecular simulations—nearly planar geometry (**b**) and TPPS in the saddle conformation (**c**)

with TPPS anions. The calculations were performed for three types of structure models: (1) the complete saturation of the interlayer space by TPPS (Type 1), (2) two–phase models where a part of the interlayers was consecutively saturated with TPPS anions followed by the interlayers containing NO_3^- anions (Type 2), and finally (3) mixed TPPS and non-exchanged NO_3^- anions in the same interlayer space (Type 3). The tilted angle of TPPS anions was slightly affected by the TPPS concentration in the interlayer. In the Type 1 and Type 3 models, the tilted angle ranged from 53 to 63° and from 67 to 71°, respectively. In all cases, TPPS anions were horizontally shifted by up to one-half of the TPPS diameter. The powder XRD patterns are very similar for Type 1 and Type 3 and are characterized by sharp basal diffraction lines, while Type 2 exhibits splitting of the diffraction lines depending on the saturation of the supercell by TPPS anions. This splitting can cause broadening of the diffraction lines. The comparison of sublimation energy characteristics of Type 2 and Type 3 models with 75% saturation by TPPS (i.e., the value close to the experimental loading) revealed that the Type 3 model is energetically less favorable. Hence, we suggest that the most probable arrangement of interlayers in partially exchanged samples is of Type 2, with consecutive interlayers saturated by TPPS anions and the remaining interlayers containing NO_3^- anions.

Acknowledgments This work was supported by the Ministry of Education, Youth and Sports of the Czech Republic (MSM 0021620835 and MSM 6046137302), the Czech Science Foundation (203/06/1244, 202/05/H003 and 205/08/0869), and the Grant Agency of the Academy of Sciences of the Czech Republic (KAN 100500651). The authors thank Petr Bezdička (Institute of Inorganic Chemistry AS CR, v.v.i.) for measuring the powder XRD patterns of the prepared samples.

References

1. Rives V (ed) (2001) Layered double hydroxides: present and future. Nova Science, New York, pp 251–411
2. Wypych F, Satyanarayana KG (2004) (eds) Clay surfaces: fundamentals and application. Elsevier, pp 374–546
3. Cavani F, Trifiro F, Vaccari A (1991) Hydrotalcite-type anionic clays: preparation, properties and applications. Catal Today 11:173–301. doi:10.1016/0920-5861(91)80068-K
4. Kovanda F, Jirátová K, Kalousková R (2006) Synthetic hydrotalcite-like compounds. In: Gerard FL (ed) Advances in chemistry research, vol 1. Nova Science, New York, pp 89–139
5. Lang K, Bezdička P, Bourdelande JL, Hernando J, Jirka I, Káfuňková E, Kovanda F, Kubát P, Mosinger J, Wagnerová DM (2007) Layered double hydroxides with intercalated porphyrins as photofunctional materials: subtle structural changes modify singlet oxygen production. Chem Mater 19:3822–3829. doi:10.1021/cm070351d
6. Del Hoyo C (2007) Layered double hydroxides and human health: an overview. Appl Clay Sci 36:103–121. doi:10.1016/j.clay.2006.06.010
7. Kim JY, Choi SJ, Oh JM, Park T, Choy JH (2007) Anticancer drug-inorganic nanohybrid and its cellular interaction. J Nanosci Nanotechnol 7:3700–3705, PMID: 18047040
8. Acharya H, Srivastava SK, Bhowmick AK (2007) Synthesis of partially exfoliated EPDM/LDH nanocomposites by solution intercalation: structural characterization and properties. Compos Sci Technol 67:2807–2816. doi:10.1016/j.compscitech.2007.01.030
9. Costa FR, Saphianikova M, Wagenknecht U, Heinrich G (2007) Layered double hydroxide based polymer nanocomposites. Adv Polym Sci 210:101–168, ISSN: 0065-3195
10. Greenwell HC, Jones W, Coveney PV, Stackhouse S (2006) On the molecular modeling of the structure and properties of clays: a materials chemistry perspective. J Mater Chem 16:708–723. doi:10.1039/b506932g
11. Kumar PP, Kalinichev AG, Kirkpatrick RJ (2006) Molecular dynamics simulation of the energetics and structure of layered double hydroxides intercalated with carboxylic acids. J Phys Chem C 111:13517–13523. doi:10.1021/jp0732054
12. Newman SP, Cristina TD, Coveney PV (2002) Molecular dynamics simulation of cationic and anionic clays containing amino acids. Langmuir 18:2933–2939. doi:10.1021/1a0114528
13. Bonnet S, Forano C, De Roy A, Besse JP, Maillard P, Momenteau M (1996) Synthesis of hybrid organo-mineral materials: anionic tetraphenylporphyrins in layered double hydroxides. Chem Mater 8:1962–1968. doi:10.1021/cm960020t
14. Marques HM, Brown KL (2002) Molecular mechanics and molecular dynamics simulations of porphyrins, metalloporphyrins, heme proteins and cobalt corrinoids. Coord Chem Rev 225:123–158. doi:10.1016/S0010-8545(01)00411-8
15. Wang J, Kalinichev AG, Kirkpatrick RJ, Hou X (2006) Effects of substrate structure and composition of the structure, dynamics, and energetics of water at mineral surfaces: a molecular modeling study. Geochim Cosmochim Acta 70:562–582. doi:10.1016/j.gca.2005.10.006
16. Kim N, Kim Y, Tsotsis TT, Sahimi M (2005) Atomistic simulation of nanoporous layered double hydroxide materials and their properties. I. Structural modeling. J Chem Phys 122:214713. doi:10.1063/1.1902945
17. Lang K, Mosinger J, Wagnerová DM (2004) Photophysical properties of porhyrinoid senzitizers non-covalently bound to host molecules; models for photodynamic therapy. Coord Chem Rev 248:321–350. doi:10.1016/j.ccr.2004.02.004
18. Lang K, Kubát P, Mosinger J, Bujdák J, Hof M, Janda P, Sýkora J, Iyi N (2008) Photoactive oriented films of layered double hydroxides. Phys Chem Chem Phys 10:4429–4434, PMID: 18654682
19. Kanezaki E, Kinugawa K, Ishikawa Y (1994) Conformation of intercalated aromatic molecular anions between layers of Mg/Al- and Zn/Al- hydrotalcites. Chem Phys Lett 226:325–330. doi:10.1016/0009-2614(94)00734-9
20. Barbosa CAS, Ferreira AMDC, Constantino VRL, Coelho ACV (2002) Preparation and characterization of Cu(II) phtalocyanine tetrasulfonate intercalated and supported on layered double hydroxides. J Incl Phenom Macrocycl Chem 42:15–23. doi:10.1023/A:1014598231722
21. Barbosa CAS, Ferreira AMDC, Constantino VRL (2005) Synthesis and Characterization of Magnesium-Aluminium Layered Double Hydroxides Containing (Tetrasulfonated porphyrin)cobalt. Eur J Inorg Chem 2005:1577–1584. doi:10.1002/ejic.200400875
22. Sazanovich IV, Galievsky VA, van Hoek A, Schaafsma TJ, Malinovskii VL, Holten D, Chirvony VS (2001) Photophysical and structural properties of saddle-shaped free base porphyrins: evidence for an "orthogonal" dipole moment. J Phys Chem B 105:7818–7829. doi:10.1021/jp010274o
23. Comba P, Hambley TW (1995) Molecular modeling of inorganic compounds. VCH, Weinheim
24. Accelrys Software (2003) Materials studio modeling environment, Release 4.3 documentation. Accelrys Software Inc, San Diego

25. Sideris PJ, Nielsen UG, Gan Z, Grey CP (2008) Mg/Al ordering in layered double hydroxides revealed by multinuclear NMR spectroscopy. Science 321:113–117. doi:10.1126/science.1157581
26. Rappé AK, Casewit CJ, Colwell KS, Goddard WA III, Skiff WM (1992) UFF, a rule-based full periodic table force field for molecular mechanics and molecular dynamics simulations. J Am Chem Soc 114:10024–10035. doi:10.1021/ja00051a040
27. Mayo SL, Olafson BD, Goddard WA III (1990) Dreiding: a generic force field for molecular simulations. J Phys Chem 94:8897–8909. doi:10.1021/j100389a010
28. Maple JR, Hwang MJ, Stockfisch TP, Dinur U, Waldman M, Ewig CS, Hagler AT (1994) Derivation of class II force fields. I. Methodology and quantum force field for the alkyl functional group and alkane molecules. J Comput Chem 15:162–182. doi:10.1002/jcc.540150207
29. Hwang MJ, Stockfisch TP, Hagler AT (1994) Derivation of class II force fields. 2. Derivation and characterization of a Class II Force Field, CFF93, for the alkyl functional group and alkane molecules. J Am Chem Soc 116:2515–2525. doi:10.1021/ja00085a036
30. Sun H, Mumby SJ, Maple JR, Hagler AT (1994) An ab initio CFF93 all-atom force field for polycarbonates. J Am Chem Soc 116:2978–2987. doi:10.1021/ja00086a030
31. Costantino U, Coletti N, Nochcetti M (1999) Anion exchange of methyl orange into Zn-Al synthetic hydrotalcite and photophysical characterization of the intercalates obtained. Langmuir 15:4454–4460. doi:10.21/la981672u
32. Miyata S (1983) Anion-exchange properties of hydrotalcite-like compounds. Clays Clay miner 31:305–311
33. Rappe AK, Goddard WA III (1991) Charge equilibration for molecular dynamics simulations. J Phys Chem 95:3358–3363. doi:10.1021/j100161a070
34. Karasawa N, Goddard WA (1989) Acceleration of convergence for lattice sums. J Phys Chem 93:7320–7327. doi:10.1021/j100358a012
35. Lennard-Jones JE (1925) Proc R Soc Lond, series A 109(752):584–597
36. Thyveetil MA, Coveney PV, Greenwell HC, Suter JL (2008) Computer simulation study of the structural stability and materials properties of DNA-intercalated layered double hydroxides. J Am Chem Soc 130:4742–4756. doi:10.1021/ja077679s